Soft tissue ossification and condylar cartilage degeneration following TMJ disc perforation in a rabbit pilot study

Mildred C. Embree[1,*], **George M. Iwaoka**[1], **Danielle Kong**[1], **Brittany N. Martin**[1], **Ryan K. Patel**[1], **Andrew Lee**[2], **John M. Nathan**[1], **Sidney B. Eisig**[1], **Aram Safarov**[3], **David A Koslovsky**[1], **Alia Koch**[1], **Alex Romanov**[3], and **Jeremy J Mao**[1]

George M. Iwaoka: giwaoka@u.rochester.edu; Danielle Kong: dankon101@gmail.com; Brittany N. Martin: bnm2107@cumc.columbia.edu; Ryan K. Patel: rkp2118@cumc.columbia.edu; Andrew Lee: al2658@cumc.columbia.edu; John M. Nathan: jmn2156@cumc.columbia.edu; Sidney B. Eisig: sbe2002@columbia.edu; Aram Safarov: as2159@cumc.columbia.edu; David A Koslovsky: dak2019@cumc.columbia.edu; Alia Koch: ak2045@cumc.columbia.edu; Alex Romanov: ar2772@cumc.columbia.edu; Jeremy J Mao: jm2654@cumc.columbia.edu

[1]College of Dental Medicine, Columbia University Medical Center, New York NY

[2]College of Physicians and Surgeons, Columbia University Medical Center, New York, NY

[3]Institute of Comparative Medicine, Columbia University Medical Center, New York, NY

Abstract

Objective—There are limited clinical treatments for temporomandibular joint pathologies, including degenerative disease, disc perforation and heterotopic ossification. One barrier hindering the development of new therapies is that animal models recapitulating TMJ diseases are poorly established. The objective of this study was to develop an animal model for TMJ cartilage degeneration and disc pathology, including disc perforation and soft tissue heterotopic ossification.

Methods—New Zealand white rabbits (n=9 rabbits) underwent unilateral TMJ disc perforation surgery and sham surgery on the contralateral side. A 2.5 mm defect was created using a punch biopsy in rabbit TMJ disc. The TMJ condyles and discs were evaluated macroscopically and histologically after 4, 8 and 12 weeks. Condyles were blindly scored by 4 independent observers using OARSI recommendations for macroscopic and histopathological scoring of osteoarthritis in rabbit tissues.

*Corresponding author: Columbia University Medical Center, P&S 16-440, 630 W 168th St, New York, NY 10032, Phone: 212-342-0677, mce2123@cumc.columbia.edu.

Results—Histological evidence of TMJ condylar cartilage degeneration was apparent in experimental condyles following disc perforation relative to sham controls after 4 and 8 weeks, including surface fissures and loss of Safranin O staining. At 12 weeks, OARSI scores indicated experimental condylar cartilage erosion into the subchondral bone. Most strikingly, heterotopic ossification occurred within the TMJ disc upon perforation injury in 6 rabbits after 8 and 12 weeks.

Conclusion—We report for the first time a rabbit TMJ injury model that demonstrates condylar cartilage degeneration and disc ossification, which is indispensible for testing the efficacy of potential TMJ therapies.

Keywords

TMJ; fibrocartilage; surgical osteoarthritis model; heterotopic ossification

INTRODUCTION

The temporomandibular joint (TMJ) is a growth center in the developing mandible (1) and is critical for chewing, breathing and speaking (2). Unlike knee articular cartilage, both the disc and condyle surface are classified as fibrocartilage (3). The pathological conditions affecting the TMJ include temporomandibular disorders (TMDs), inflammatory and degenerative diseases and traumatic injuries (2). TMJ disc perforation has been associated in patients with TMJ osteoarthritis (OA) (4,5), rheumatic/inflammatory disease (6), and internal disc derangement (7); however, whether TMJ disc perforations in humans cause pain or degeneration is unclear. Heterotopic ossifications (HO) within the TMJ synovial space and also within TMJ soft tissue are prevalent among children with juvenile idiopathic arthritis (8), adults with chronic TMD (9), patients undergoing TMJ surgery/injury (10) and with TMJ disc perforations (11). Given that multiple TMJ tissues can be affected pathologically, including the condyle and disc, the development of effective total joint treatments has been challenging. Furthermore, the availability of preclinical animal models that recapitulate the complexity of human TMJ pathologies is limited. Our goal was to develop a pre-clinical animal model for TMJ cartilage degeneration and disc pathology, including disc perforation and soft tissue heterotopic ossification.

Heterotopic ossification is characterized by endochondral bone formation in soft musculoskeletal tissue, including muscle, tendon, and ligament (12), and may either be genetically inherited, such as fibrodysplasia ossificans progressive (13), or acquired following trauma (12,14,15). Given that TMJ HO has been associated with TMJ disc perforations (11) and HO has been associated with trauma in other musculskeletal tissues (12, 14–16), we proposed that TMJ disc injury could induce HO. To test this hypothesis, we created a 2.5 mm perforation in the TMJ disc using New Zealand white rabbits. We analyzed the TMJ disc and condyle phenotype after 4, 8 and 12 weeks. While great strides have been made to standardize OA model analyses for the knee joint in multiple species (17), it has not been applied to the TMJ, a non weight-bearing joint. Therefore, we also applied OARSI recommendations for the systematic histopathological assessment of OA in a rabbits (18). We discovered that TMJ condyle degeneration was evident in the rabbit condyle following disc perforation and OARSI systematic scoring reflected severe

histopatholgical evidence of osteoarthritis by 12 weeks, including ulceration and cartilage erosion to the bone. Most strikingly, we also observed evidence of bone formation within the TMJ disc in this model following TMJ disc perforation injury after 8 and 12 weeks. To corroborate our *in vivo* findings, we provide further evidence that rabbit TMJ disc cells are capable of calcification *in vitro*. We report for the first time a rabbit TMJ injury model that demonstrates condylar cartilage degeneration and disc ossification, which is critical for testing potential TMJ therapies.

MATERIALS AND METHODS

Animals

All animal procedures were performed with approval from the Animal Care and Use Committee, Columbia University Medical Center (protocol #AC-AAAD9804).

TMJ Injury Model

TMJ injury was surgically induced in a total of 9 New Zealand white rabbits 3–4 months old. An oblique incision was created superior to the zygomatic process. Tissue was elevated and retracted to access the TMJ superior joint space and the disc was retracted posteriorly. A periosteal elevator was placed under the disc to protect the condyle from injury. A punch biopsy was used to create a 2.5 mm perforation in the lateral portion of the TMJ disc. No disc attachments were severed and the disc reduced to its normal anatomical location upon release of disc retraction. Sham surgery was performed on the contralateral side, the TMJ superior joint space was accessed, and the disc was not perforated. A total of 3 rabbits were randomly euthanized per time point at 4, 8 and 12 weeks after surgery for macroscopic and histological evaluation.

Macroscopic Evaluation

TMJ images were captured using a Nikon DS-Fi2 microscope. The anterior to posterior (AP) length and perforation size were measured using Nis-Elements Basic Research Imaging software. To standardize medial to lateral (ML) measurements, the ML width of each condyle and disc was measured precisely at the midpoint of the AP length. Xray images were captured using Kodak *in vivo* Multispectral Imaging Station. A total of 4 observers blindly scored macroscopic changes in the articular surface of the TMJ condyles at the 12-week time point (n= 3 rabbits) (18) (Supplemental Table 1).

Scanning electron microscopy

Samples were fixed overnight in 5% glutaraldehyde, post-fixed in 2% osmium tetroxide for 1 hour, dehydrated in a graded series of ethanol (25%–100%), dried to critical point in liquid CO_2, mounted and coated with gold. FEI Quanta 200 3D scanning electron microscope was used to image comparable locations on TMJ condyle surface.

Histological Analysis and Semi-quantitative Evaluation

TMJs were fixed for 3 days in 4% paraformaldehyde, washed in tap water, and decalcified in 0.5 M EDTA for 12 weeks. Specimens were classically processed for histology,

embedded in paraffin and sectioned. Serial sections were stained by hematoxylin and eosin (H&E) and by Safranin O/fast green. OARSI recommendations for a histological scoring system was used to semi-quantitate histological changes at the 12 week time point, in the experimental TMJs *versus* the sham TMJs (n=3 rabbits). Four observers blindly the TMJ structure, cell density, cluster formation, and safranin O staining using comparable histological sections. (18) (Supplemental Table 2).

Cell Culture and Mineralization Assay

TMJ discs were dissected from 2 New Zealand white rabbit 3-months old and digested in dispase II/collagenase I (4mg/ml/3mg/ml) for 45 minutes at 37°C. Single-cell suspensions were cultured (5% CO_2, 37°C) in DMEM (Invitrogen 11885-092) supplemented with 20% lot-selected fetal bovine serum, glutamax (Invitrogen 35050-061), penicillin-streptomycin (Invitrogen 15140-163), and 100 mM 2-mercaptoethanol (Gibco) for 4–6 days. Cells were cultured in osteogenic media with 100ng/ml BMP2 (R&D 355-BM-050) for 2 weeks and compared to basal medium controls. Calcium nodules were stained with 2% alizarin red. Alizarin red was solubilized with 5% SDS in 0.5 N HCl. Absorbance was measured at 405 nm and normalized to cell number using Cell Counting Kit-8 (Dojindo CK04-05).

Real Time PCR

Total RNA was purified from TMJ disc cells using PureLLink™ RNA Mini Kit (Ambion 12183018A) and RNA was treated with DNAse I (Ambion AM2222). RNA quantity and purity was determined using Nanodrop™ spectrophotometer. RNA samples (260/280>1.8) were used to obtain cDNA (Biorad AM2222). Quantitative RT-PCR was performed using TaqMan® Universal PCR Master Mix (Applied Biosystems 4304437) and *runx2* TaqMan® Gene Expression Assay (Applied Biosystems Oc02386741_m1). Gene expression levels were normalized to housekeeping gene *gapdh* TaqMan® Gene Expression Assay (Applied Biosystems Rn01775763_g1*).

Statistical Analysis

A total of 9 rabbits underwent unilateral disc perforation surgery and contralateral sham surgery served as control. Rabbits were randomly divided for SEM after 4 (n=1 rabbit) and 8 weeks (n= 1 rabbit) and histology after 4 (n=2 rabbits), 8 (n = 2 rabbits) and 12 weeks (n=3 rabbits). For OARSI histological scoring, 4 observers blindly scored experimental and sham TMJs (n=3 rabbits) at the 12-week time point. Macroscopic score for each rabbit is represented as a mean (n=4 observers) with 95% confidence intervals and the overall score is represented as a mean (n=3 rabbits) with 95% confidence intervals. Each observer OARSI histological score per rabbit was obtained based on mean of 3 different sections of the same condyle. An overall mean score was obtained per rabbit for each OARSI histological grading parameter with 95% confidence intervals (n=4 observers). Overall OARSI scores at 12 weeks are reported as a mean with 95% confidence intervals (n= 3 rabbits). For TMJ dimensions (n=9 rabbits), real time PCR (n=6 independent experiments), and alizarin red quantification (n=5 independent experiments), values are representative as mean with 95% confidence intervals. Normality of distribution was confirmed using Kolmogorov-Smirnov test and the statistical significance of differences was determined using paired Student's t-

test assuming Gaussian distribution using Prism 6 Graphpad Software. Resulting two-tailed P-value 0.05 was regarded as statistically significant difference.

RESULTS

Surgical TMJ disc perforation in New Zealand white rabbits

Previous studies demonstrated that TMJ demise occurs over a 24-week time point by generating a 1.6 mm defect in rabbit TMJ disc (20). We proposed a larger perforation size would shorten the time for TMJ demise for economic drug screening and testing of bioengineered tissue replacements. Thus, we selected a 2.5 mm perforation size for these studies. Given that the rabbit TMJ disc is ~3.0–3.5 mm wide, 2.5 mm perforation was the largest perforation that could be surgically created accurately without completely severing the disc. An oblique incision was made superior to the zygomatic process (Fig. 1a, red line). Tissue was elevated and retracted to access the TMJ superior joint space behind the zygomatic process and forceps were used to retract the disc posteriorly (Fig. 1b). A periosteal elevator was placed under the disc to prevent damage to the underlying TMJ condyle. A punch biopsy was used to create a 2.5 mm defect within the posterior-lateral portion of the TMJ disc (Fig. 1c) and no TMJ disc attachments were severed. The perforated tissue was excised (Fig. 1d) and the surgical incision was closed with both internal and external sutures. A sham procedure was performed on the contralateral side, whereby the TMJ disc was exposed and accessed, but no perforation was performed. Rabbits were fed a soft gruel for 1–3 days followed by a normal diet. No changes occurred in dietary habits or total mass. Rabbits were divided randomly and euthanized after 4, 8 and 12 weeks.

Macroscopic changes in condyle in rabbit TMJ injury model

Macroscopic changes in TMJ condyles were also analyzed at 4, 8 and 12 weeks after surgery (Fig. 2). In the TMJ injury condyle at 4 weeks, gross morphological examination revealed widespread irregular surface relative to sham control and appeared slightly swollen (Fig. 2a, top panels). By 8 weeks, TMJ condyle appeared inflamed, erythmatic with severely irregular surface. Experimental condyles began to show early signs of cartilage erosion and notably swollen relative to sham control (Fig. 2a, middle panels). At 12 weeks, TMJ condyles were dysmorphic and showed ulceration and erosion over the entire joint surface and condylar swelling (Fig. 2a). To confirm the swelling in the experimental condyles, we measured the medial to lateral widths compared to sham controls (Fig. 2b). The medial to lateral width of experimental condyles were 2 mm greater compared to sham controls (Fig. 2b, p=0.001, n=9 rabbits).

Based on our gross macroscopic analysis of the TMJ condyles, we proposed that the experimental TMJ condyle displayed fibrillation on the articular surface of the fibrocartilage tissue lining the surface. We then used scanning electron microscopy (SEM) to visualize the fibrillation on the fibrocartilage surface of the TMJ condyles at 4 and 8 weeks. SEM demonstrated breaks within the surface collagen fibers and surface irregularity in the fibrocartilage tissue at 4 weeks in comparison to the smooth surface on the sham control condyle (Fig. 3). By 8 weeks, the surface roughness and irregularity was more pronounced and widespread (Fig. 3). Taken together these SEM images correspond to our macroscopic

findings demonstrating increasing surface irregularities and erosion in the experimental TMJ condyles in comparison to the sham control side.

TMJ condyle degeneration in rabbit TMJ injury model

To corroborate our macroscopic observations, we performed a histological evaluation of H&E and Safranin O stainings for proteoglycan content of the TMJ condyles (Fig. 4). At 4 and 8 weeks, experimental condyles displayed classical histopathological features of osteoarthritis (3,21,22), including surface irregularities and fissures (black triangles), a multifocal decrease in cells (asterisks), and the formation of chondrocyte clusters (black arrows) (Fig. 4a, top and middle panels). Experimental condyles were significantly thicker than sham at 4 and 8 weeks (Supplemental Fig. 1a, p=0.01, n=6 rabbits). In parallel to the structural/cellular changes, we also observed diffuse Safranin O staining and a loss of staining ranging in the upper 1/3 – 2/3 of the condyle (Fig. 4b). The most severe osteoarthritic changes in the condylar cartilage were evident at 12 weeks after surgery (Fig. 4a–b, bottom panels). Structural changes included full depth erosion (red arrows) and calcified cartilage down to the subchondral bone and a widespread loss of cells (asterisks) (Fig. 4a, bottom panels). Most of the cells that were present at 12 weeks existed within a cluster of 3 or more cells (black arrows). Given the cartilage erosion that occurred, it is not surprising that we also observed complete loss of safranin O staining at 12 weeks, suggesting loss of proteoglycan content in experimental TMJs (Fig. 4b, bottom panels). Interestingly, we noted the greatest proteoglycan loss occurred with the mid-anterior portion of the condyle, which could be due to condylar regional differences in proteoglycan content and changes in biomechanical loading and joint instability upon disc perforation injury (23). The contralateral TMJs within the same animal maintained tissue condyle architecture and uniform distribution of Safranin staining, suggesting that contralateral TMJs were not affected by the unilateral disc perforation surgery (Figs. 4a–b, right columns).

OARSI Histopathological Scoring

To further confirm the osteoarthritic changes in our model, we used OARSI recommendations for a macroscopic and histological scoring system (18) (Supplemental Tables 1–2). Given that we anticipate using this model to test TMJ regenerative therapies using bioengineered constructs, we analyzed 12-week time point to confirm the observed loss of cartilage tissue. A total of 4 observers blindly scored macroscopic changes (Fig. 5a, b) and comparable histological sections based on structure (Fig. 5c, d), cell density (Fig. 5e, f), cellular cluster formation (Fig. 5g, h) and Safranin O staining (Fig. 5i, j) in the experimental condyles and the contralateral sham condyles in 3 rabbits 12 weeks following disc perforation surgery.

For macroscopic evaluation, each observer scored the experimental condyles in a range from 6–8 and at least two of the observers were in agreement, while the sham control scores ranged from 0–1 (Fig. 5a). The experimental condyle had a mean macroscopic score of 7, indicating ulcerative changes. However, the sham controls ranked an average score of less than 1, reflecting normal scores (Fig. 5b). The observers ranked experimental condyles structure in the range from 8–11 (full depth erosion in at least 50% of surface), while sham controls scores ranged from 0–1 (normal to mild surface irregularities) (Fig. 5c). At 12

weeks, average experimental condyle structure score was 9.5 and noted full depth erosion hyaline and calcified cartilage to the subchondral bone. On the other hand, sham control average score at 12 weeks was ranked on average at 1, representing surface irregularity (Fig. 5d). At least 3 observers were in agreement with experimental cell density scores (Fig. 5e–f) with experimental condyle scores ranging from 3–4 (multifocal to diffuse loss of cells) and sham condyles ranging from 0–1 (no to focal decrease in cells). Cell cluster scores showed the most range in individual observer's scores with sham condyle scores ranging between 0–3 and experimental condyles ranging from 1–3 (Fig. 5g). Average cluster formation scores ranked between 1–2 for experimental and sham controls (Fig. 5h), which may be due an overall loss of cells at this time point. Experimental condyle Safranin O scores ranged within 2 values (4–6, loss of Safranin O staining in upper 2/3 cartilage to all of cartilage) (Fig. 5i). Mean experimental Safranin O scores ranked at mean of 5 while, mean sham controls ranked less than 1 (Fig. 5j). Overall, observers ranked mean OARSI scores for experimental condyles as indicative of degenerative pathology.

Heterotopic bone formation in TMJ disc in rabbit TMJ injury model

Rabbit TMJ discs from the experimental side were compared to the contralateral TMJ disc in the same rabbit (Fig. 6). The experimental TMJ discs were larger than sham disc within the same animal (Fig. 6a–c, Supplemental Fig. 1b). The medial to lateral width (Fig. 6b, p=0.0001), anterior to posterior length (Fig. 6c, p=0.0009, n=9 rabbits), and thickness (Supplemental Fig. 1c, p=0.0001, n=9 rabbits) was significantly greater in the experimental discs relative to the sham discs. These data suggested experimental discs underwent hyperplasia and fibrosis. The defect in TMJ discs that underwent perforation surgery was apparent and did not close at the latest time point 12 weeks (Fig. 6a). There were no significant changes in perforation size (Supplemental Fig. 1c). Radiographic examination of TMJ discs showed all the experimental TMJ discs at 8 and 12 weeks displayed radiopaque tissue within the borders of the perforation site (Fig. 6d, yellow arrows), suggesting the presence of radiopaque, mineralized tissue.

At 4 weeks sham discs showed Safranin O staining uniformly distributed (Supplemental Fig. 2a, right) and localized between elongated collagen fibers (Supplemental Fig. 2b, right) (24, 25). However, experimental discs showed altered Safranin O staining, where proteoglycan content was re-distributed and localized within the perforation tissue border (Supplemental Fig. 2a, left) and also had disorganized collagen fibers (Supplemental Fig. 2b left). At 8 (not shown) and 12 weeks, histology corroborated the presence of bone-like tissue formed within the fibrous TMJ disc tissue surrounding the perforation site in the experimental TMJ disc (Fig. 6e, left panels). TMJ disc cells were embedded in a lacunae and trabecular bone-like matrix with areas of bone marrow-like spaces (Fig. 6e, left bottom panel). On the other hand, sham TMJ discs maintained classic disc morphology (24,25) (Fig. 6e, right panels), whereby TMJ disc cells were embedded between elongated, collagen fibers (Fig. 6e, right panel, arrows). Altogether, our histological evaluation suggested that endochondral bone formation occurred. We further tested whether TMJ disc cells were capable of mineralizing by culturing TMJ disc cells in osteogenic media. Alizarin staining demonstrated that TMJ disc cells formed calcium nodules in the presence of osteogenic media (Fig. 6f, red) and was significantly higher than cells cultured in basal media controls (p=0.0002, Fig. 6g). We

examined the expression of *runx2* by real time PCR, given *runx2* is an early bone marker that is upregulated in heterotopic ossification of other soft tissues (15,26). Compared to TMJ disc cells in basal media, *runx2* upregulated by 13.5 fold in TMJ disc cells in osteogenic media (Fig. 6h). Taken together, our data suggest that TMJ disc cells may be promoted to form heterotopic endochondral bone upon perforation injury.

DISCUSSION

We present a surgical rabbit TMJ disc perforation model demonstrating cellular and histological evidence that signify cartilage degeneration and disc ossification. Our macroscopic analysis demonstrated experimental TMJ condyles showed widespread surface irregularities at 4 weeks and complete erosion/ulceration by 12 weeks. Macroscopic changes were coupled with a 2 mm increase in condyle width, likely resulting from inflammation that we will continue to characterize, and surface irregularities were visibly apparent under SEM. Histological analysis showed OA pathological features (21,22) at 4 and 8 weeks, including the formation of chondrocyte clusters, cartilage thickening, multifocal loss of cells, and loss of Safranin O staining in the superficial 1/3–2/3 of the condyle. By 12 weeks severe cartilage damage was evident, whereby cartilage eroded to the subchondral bone with a diffuse loss of cells and proteoglycan content. Given OARSI scoring system has only been applied to the knee (18), we applied OARSI scoring to the TMJ for the first time. We found relative consistency among observers' scores. Overall, experimental condyles had mean macroscopic, structure, cell density and Safranin O mean scores reflecting pathological and degenerative changes. However, cell cluster scores showed more variability among observers, which could be due to experimental condyles exhibiting an overall diffuse loss of cells and a lower number of chondrocyte clusters.

We showed for the first time an animal model whereby TMJ disc injury induced heterotopic ossification (HO). TMJ HO has been reported in patients that have undergone TMJ injury/ surgery (10,27,28), TMJ disc perforations (11) chronic TMD patients (29), and also in children with juvenile rheumatoid osteoarthritis (8). While TMJ HO etiology can vary, the symptomatic outcomes are the same. TMJ HO can limit TMJ range of motion, cause pain, and impact facial development in children (8,10,30–32). One plausible mechanism underlying HO is that upon musculoskeletal tissue injury, macrophages secrete potent osteoinductive signals (36), such as BMP2, local fibrosis occurs, osteoprogenitor cells migrate to the injury site and form endochondral bone (33–35) (Supplemental Text Discussion). Similarly at 4 weeks, we observed the redistribution of Safranin O staining to be concentrated around the tissue injury borders, which was also coupled with an increase in disc thickness at the site of injury, suggesting tissue fibrosis and early endochondral ossification. We further showed bone-like tissue formed after 8 and 12 weeks at the injury site. Additionally we showed rabbit TMJ disc cells undergo mineralization in the presence of BMP2 and osteogenic media. Furthermore, mechanical forces upon chewing could also stimulate local cells to undergo osteogenesis (37). Taken together, we propose that upon disc perforation inflammatory mediators recruit skeletal progenitor migration to perforation site, skeletal progenitors proliferate resulting in larger and thicker discs, progenitors differentiate into cartilage and secrete a matrix rich in GAGs, and finally the cartilage remodels into bone.

There are several plausible mechanisms underlying condylar cartilage degeneration in this model, including joint atrophy due to TMJ disuse or condyle excessive loading that is associated with OA. However, there are cartilage phenotypic differences that distinguish TMJ atrophy/disuse from TMJ overloading in OA pathology. TMJ atrophy has been tested using unloading murine models (38–40) (Supplemental Text Discussion). Murine unloading/atrophy models involve subjecting mice to soft diets and/or incisor trimming to emulate atrophy/disuse (38–40). Atrophic and TMJ disuse is characterized with an initial decrease cartilage thickness and a decrease in condyle dimensions (38–40). This is in contrast to TMJ overloading in TMJ OA pathology, where OA is marked by an increase in cartilage thickness and an increase in condyle dimensions (3,21,22). Unlike TMJ unloading/atrophic models (38–40), we observed cartilage thickening and increases in condyle dimension that preceded cartilage erosion in this model. Thus we speculate that condyle excessive loading more likely contributes to degenerative mechanisms in this rabbit disc perforation model. Interestingly, similar to TMJ OA mouse genetic models (3), in this model we also observed the depletion of cells within the superficial articular zone, which may contain a reservoir of progenitor cells (1,3). Thus, one possibility that we plan to explore is that excessive loading may cause depletion of progenitor cells in our model over time (41).

To test the efficacy of potential TMJ therapies, the development of an experimental TMJ disease animal model that emulates human TMJ pathology is crucial. Currently, there are several types of animal models demonstrating TMJ disease (42), including genetically modified mice (21,22), chemically induced inflammatory animal models (43), and surgically induced models (20,44,45). However, to our knowledge, this is the first reported animal model demonstrating both TMJ condylar cartilage degeneration and TMJ disc heterotopic bone formation. Furthermore, unlike other rabbit surgical models, condylar cartilage erosion occurs within 12 weeks as opposed to 24 (20), and is thus more economical for our plans to surgically test bioengineered TMJ replacements (46,47). We also used rabbits given the larger species size affords greater ease of surgical accuracy. Given that the anatomical and biomechanical properties of pig TMJ is most similar to humans, pigs have been widely accepted as an ideal species for studying TMJ biology and pathology (48). Unlike rabbit TMJ (49), pig TMJ is more anatomically similar to humans because pigs also have bilateral occlusion and can participate in translational/sliding movements (48). However, the daily maintenance and surgical costs for pigs for testing experimental therapies to treat TMJ disease is significantly more than in rabbits (50). Thus, we found the use of this rabbit TMJ disc perforation model offers multiple advantages, including condyle degeneration and disc ossification, relative ease of TMJ surgery and recovery, ease of daily animal care and handling, and a cost-effective experimental approach.

Supplementary Material

Refer to Web version on PubMed Central for supplementary material.

Acknowledgments

References

1. Shen G, Darendeliler MA. The adaptive remodeling of condylar cartilage---a transition from chondrogenesis to osteogenesis. Journal of dental research. 2005; 84:691–699. [PubMed: 16040724]

2. Scrivani SJ, Keith DA, Kaban LB. Temporomandibular disorders. The New England journal of medicine. 2008; 359:2693–2705. [PubMed: 19092154]

3. Embree MC, Kilts TM, Ono M, Inkson CA, Syed-Picard F, Karsdal MA, Oldberg A, Bi Y, Young MF. Biglycan and fibromodulin have essential roles in regulating chondrogenesis and extracellular matrix turnover in temporomandibular joint osteoarthritis. The American journal of pathology. 2010; 176:812–826. [PubMed: 20035055]

4. Dijkgraaf LC, Spijkervet FK, de Bont LG. Arthroscopic findings in osteoarthritic temporomandibular joints. Journal of oral and maxillofacial surgery: official journal of the American Association of Oral and Maxillofacial Surgeons. 1999; 57:255–268. discussion 269–270.

5. Cholitgul W, Petersson A, Rohlin M, Akerman S. Clinical and radiological findings in temporomandibular joints with disc perforation. International journal of oral and maxillofacial surgery. 1990; 19:220–225. [PubMed: 2120363]

6. Helenius LM, Tervahartiala P, Helenius I, Al-Sukhun J, Kivisaari L, Suuronen R, Kautiainen H, Hallikainen D, Lindqvist C, Leirisalo-Repo M. Clinical, radiographic and MRI findings of the temporomandibular joint in patients with different rheumatic diseases. International journal of oral and maxillofacial surgery. 2006; 35:983–989. [PubMed: 17052893]

7. Kondoh T, Westesson PL, Takahashi T, Seto K. Prevalence of morphological changes in the surfaces of the temporomandibular joint disc associated with internal derangement. Journal of oral and maxillofacial surgery: official journal of the American Association of Oral and Maxillofacial Surgeons. 1998; 56:339–343. discussion 343–334.

8. Ringold S, Thapa M, Shaw EA, Wallace CA. Heterotopic ossification of the temporomandibular joint in juvenile idiopathic arthritis. The Journal of rheumatology. 2011; 38:1423–1428. [PubMed: 21498479]

9. Luz JG, Rodrigues L, Chilvarquer I, Soler JM. Mineralization of stylohyoid ligament complex in patients with temporomandibular disorders and asymptomatic individuals: a comparative study. Journal of oral rehabilitation. 2003; 30:909–913. [PubMed: 12950972]

10. Lindqvist C, Soderholm AL, Hallikainen D, Sjovall L. Erosion and heterotopic bone formation after alloplastic temporomandibular joint reconstruction. Journal of oral and maxillofacial surgery: official journal of the American Association of Oral and Maxillofacial Surgeons. 1992; 50:942–949. discussion 950.

11. Jibiki M, Shimoda S, Nakagawa Y, Kawasaki K, Asada K, Ishibashi K. Calcifications of the disc of the temporomandibular joint. Journal of oral pathology & medicine: official publication of the International Association of Oral Pathologists and the American Academy of Oral Pathology. 1999; 28:413–419.

12. McCarthy EF, Sundaram M. Heterotopic ossification: a review. Skeletal radiology. 2005; 34:609–619. [PubMed: 16132978]

13. Medici D, Shore EM, Lounev VY, Kaplan FS, Kalluri R, Olsen BR. Conversion of vascular endothelial cells into multipotent stem-like cells. Nature medicine. 2010; 16:1400–1406.

14. Shimono K, Tung WE, Macolino C, Chi AH, Didizian JH, Mundy C, Chandraratna RA, Mishina Y, Enomoto-Iwamoto M, Pacifici M, Iwamoto M. Potent inhibition of heterotopic ossification by nuclear retinoic acid receptor-gamma agonists. Nature medicine. 2011; 17:454–460.

15. Lin L, Shen Q, Xue T, Yu C. Heterotopic ossification induced by Achilles tenotomy via endochondral bone formation: expression of bone and cartilage related genes. Bone. 2010; 46:425–431. [PubMed: 19735753]

16. Forsberg JA, Pepek JM, Wagner S, Wilson K, Flint J, Andersen RC, Tadaki D, Gage FA, Stojadinovic A, Elster EA. Heterotopic ossification in high-energy wartime extremity injuries: prevalence and risk factors. The Journal of bone and joint surgery American volume. 2009; 91:1084–1091. [PubMed: 19411456]

17. Berenbaum F. The OARSI histopathology initiative - the tasks and limitations. Osteoarthritis and cartilage / OARS, Osteoarthritis Research Society. 2010; 18(Suppl 3):S1.

18. Laverty S, Girard CA, Williams JM, Hunziker EB, Pritzker KP. The OARSI histopathology initiative - recommendations for histological assessments of osteoarthritis in the rabbit. Osteoarthritis and cartilage / OARS, Osteoarthritis Research Society. 2010; 18(Suppl 3):S53–65.

19. Bi Y, Ehirchiou D, Kilts TM, Inkson CA, Embree MC, Sonoyama W, Li L, Leet AI, Seo BM, Zhang L, Shi S, Young MF. Identification of tendon stem/progenitor cells and the role of the extracellular matrix in their niche. Nature medicine. 2007; 13:1219–1227.

20. Narinobou M, Takatsuka S, Nakagawa K, Kubota Y, Terai K, Yamamoto E. Histological changes in the rabbit condyle following posterolateral disk perforation. Journal of cranio-maxillo-facial surgery: official publication of the European Association for Cranio-Maxillo-Facial Surgery. 2000; 28:345–351. [PubMed: 11465142]

21. Wadhwa S, Embree MC, Kilts T, Young MF, Ameye LG. Accelerated osteoarthritis in the temporomandibular joint of biglycan/fibromodulin double-deficient mice. Osteoarthritis and cartilage / OARS, Osteoarthritis Research Society. 2005; 13:817–827.

22. Wadhwa S, Embree M, Ameye L, Young MF. Mice deficient in biglycan and fibromodulin as a model for temporomandibular joint osteoarthritis. Cells, tissues, organs. 2005; 181:136–143. [PubMed: 16612079]

23. Singh M, Detamore MS. Biomechanical properties of the mandibular condylar cartilage and their relevance to the TMJ disc. Journal of biomechanics. 2009; 42:405–417. [PubMed: 19200995]

24. Allen KD, Athanasiou KA. Tissue Engineering of the TMJ disc: a review. Tissue engineering. 2006; 12:1183–1196. [PubMed: 16771633]

25. Kalpakci KN, Willard VP, Wong ME, Athanasiou KA. An interspecies comparison of the temporomandibular joint disc. Journal of dental research. 2011; 90:193–198. [PubMed: 21118792]

26. Iwasaki M, Piao J, Kimura A, Sato S, Inose H, Ochi H, Asou Y, Shinomiya K, Okawa A, Takeda S. Runx2 haploinsufficiency ameliorates the development of ossification of the posterior longitudinal ligament. PloS one. 2012; 7:e43372. [PubMed: 22927960]

27. Guarda-Nardini L, Manfredini D, Olivo M, Ferronato G. Long-Term Symptoms Onset and Heterotopic Bone Formation around a Total Temporomandibular Joint Prosthesis: a Case Report. Journal of oral & maxillofacial research. 2014; 5:e6. [PubMed: 24800055]

28. Wolford LM, Cottrell DA, Henry CH. Temporomandibular joint reconstruction of the complex patient with the Techmedica custom-made total joint prosthesis. Journal of oral and maxillofacial surgery: official journal of the American Association of Oral and Maxillofacial Surgeons. 1994; 52:2–10. discussion 11.

29. Kuribayashi A, Okochi K, Kobayashi K, Kurabayashi T. MRI findings of temporomandibular joints with disk perforation. Oral surgery, oral medicine, oral pathology, oral radiology, and endodontics. 2008; 106:419–425.

30. Shibuya T, Kino K, Kitamura Y, Takahashi T. Synovial osteochondromatosis accompanying an ossified articular disk in the temporomandibular joint: a case report. Journal of oral pathology & medicine: official publication of the International Association of Oral Pathologists and the American Academy of Oral Pathology. 2003; 32:441–442.

31. Koyama J, Ito J, Hayashi T, Kobayashi F. Synovial chondromatosis in the temporomandibular joint complicated by displacement and calcification of the articular disk: report of two cases. AJNR. American journal of neuroradiology. 2001; 22:1203–1206. [PubMed: 11415920]

32. Jensen AW, Viozzi CF, Foote RL. Long-term results of radiation prophylaxis for heterotopic ossification in the temporomandibular joint. Journal of oral and maxillofacial surgery: official journal of the American Association of Oral and Maxillofacial Surgeons. 2010; 68:1100–1105.

33. Kan L, Liu Y, McGuire TL, Berger DM, Awatramani RB, Dymecki SM, Kessler JA. Dysregulation of local stem/progenitor cells as a common cellular mechanism for heterotopic ossification. Stem cells. 2009; 27:150–156. [PubMed: 18832590]

34. Ji Y, Christopherson GT, Kluk MW, Amrani O, Jackson WM, Nesti LJ. Heterotopic ossification following musculoskeletal trauma: modeling stem and progenitor cells in their microenvironment. Advances in experimental medicine and biology. 2011; 720:39–50. [PubMed: 21901617]

35. Shahab-Osterloh S, Witte F, Hoffmann A, Winkel A, Laggies S, Neumann B, Seiffart V, Lindenmaier W, Gruber AD, Ringe J, Haupl T, Thorey F, Willbold E, Corbeau P, Gross G. Mesenchymal stem cell-dependent formation of heterotopic tendon-bone insertions (osteotendinous junctions). Stem cells. 2010; 28:1590–1601. [PubMed: 20882636]

36. Champagne CM, Takebe J, Offenbacher S, Cooper LF. Macrophage cell lines produce osteoinductive signals that include bone morphogenetic protein-2. Bone. 2002; 30:26–31. [PubMed: 11792561]

37. Kelly DJ, Jacobs CR. The role of mechanical signals in regulating chondrogenesis and osteogenesis of mesenchymal stem cells. Birth defects research Part C, Embryo today: reviews. 2010; 90:75–85.

38. Chen J, Sorensen KP, Gupta T, Kilts T, Young M, Wadhwa S. Altered functional loading causes differential effects in the subchondral bone and condylar cartilage in the temporomandibular joint from young mice. Osteoarthritis and cartilage / OARS, Osteoarthritis Research Society. 2009; 17:354–361.

39. Chen J, Sobue T, Utreja A, Kalajzic Z, Xu M, Kilts T, Young M, Wadhwa S. Sex differences in chondrocyte maturation in the mandibular condyle from a decreased occlusal loading model. Calcified tissue international. 2011; 89:123–129. [PubMed: 21597908]

40. Pirttiniemi P, Kantomaa T, Salo L, Tuominen M. Effect of reduced articular function on deposition of type I and type II collagens in the mandibular condylar cartilage of the rat. Archives of oral biology. 1996; 41:127–131. [PubMed: 8833602]

41. Responte DJ, Lee JK, Hu JC, Athanasiou KA. Biomechanics-driven chondrogenesis: from embryo to adult. FASEB journal: official publication of the Federation of American Societies for Experimental Biology. 2012; 26:3614–3624. [PubMed: 22673579]

42. Ameye LG, Young MF. Animal models of osteoarthritis: lessons learned while seeking the "Holy Grail". Current opinion in rheumatology. 2006; 18:537–547. [PubMed: 16896297]

43. Harper RP, Kerins CA, McIntosh JE, Spears R, Bellinger LL. Modulation of the inflammatory response in the rat TMJ with increasing doses of complete Freund's adjuvant. Osteoarthritis and cartilage / OARS, Osteoarthritis Research Society. 2001; 9:619–624.

44. Lang TC, Zimny ML, Vijayagopal P. Experimental temporomandibular joint disc perforation in the rabbit: a gross morphologic, biochemical, and ultrastructural analysis. Journal of oral and maxillofacial surgery: official journal of the American Association of Oral and Maxillofacial Surgeons. 1993; 51:1115–1128.

45. Hagandora CK, Almarza AJ. TMJ disc removal: comparison between pre-clinical studies and clinical findings. Journal of dental research. 2012; 91:745–752. [PubMed: 22744995]

46. Alhadlaq A, Mao JJ. Tissue-engineered neogenesis of human-shaped mandibular condyle from rat mesenchymal stem cells. Journal of dental research. 2003; 82:951–956. [PubMed: 14630893]

47. Lee CH, Cook JL, Mendelson A, Moioli EK, Yao H, Mao JJ. Regeneration of the articular surface of the rabbit synovial joint by cell homing: a proof of concept study. Lancet. 2010; 376:440–448. [PubMed: 20692530]

48. Herring SW, Decker JD, Liu ZJ, Ma T. Temporomandibular joint in miniature pigs: anatomy, cell replication, and relation to loading. The Anatomical record. 2002; 266:152–166. [PubMed: 11870598]

49. Langenbach GE, Weijs WA. Growth patterns of the rabbit masticatory muscles. Journal of dental research. 1990; 69:20–25. [PubMed: 2303596]

50. Teeple E, Jay GD, Elsaid KA, Fleming BC. Animal models of osteoarthritis: challenges of model selection and analysis. The AAPS journal. 2013; 15:438–446. [PubMed: 23329424]
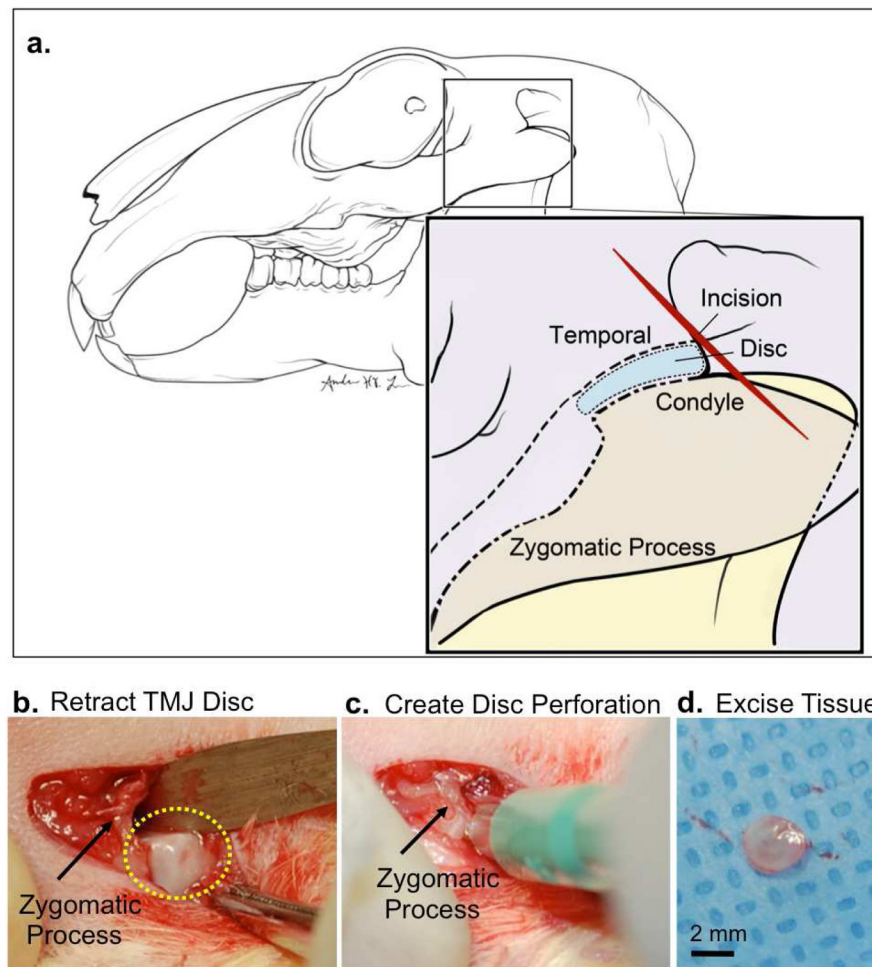
Figure 1. Rabbit TMJ injury model

New Zealand white rabbits (N=9) underwent unilateral TMJ disc perforation surgery on the left TMJ. Sham surgery was performed on the right contralateral TMJ within the same rabbit and served as a comparison control. (**a**) Diagram illustrating New Zealand white rabbit TMJ anatomy. The disc is localized behind the zygomatic process. An oblique incision was made superior to the zygomatic process. (**b**) The TMJ superior joint space was accessed and forceps were used to retract the disc (yellow dashed lines) posterior to the zygomatic process (black arrow). (**c**) A punch biopsy was used to create a 2.5 mm perforation in the anterior lateral TMJ disc. (**d**) A 2.5 mm tissue was excised from the TMJ disc and the incision was sutured. Scale bar = 2mm.
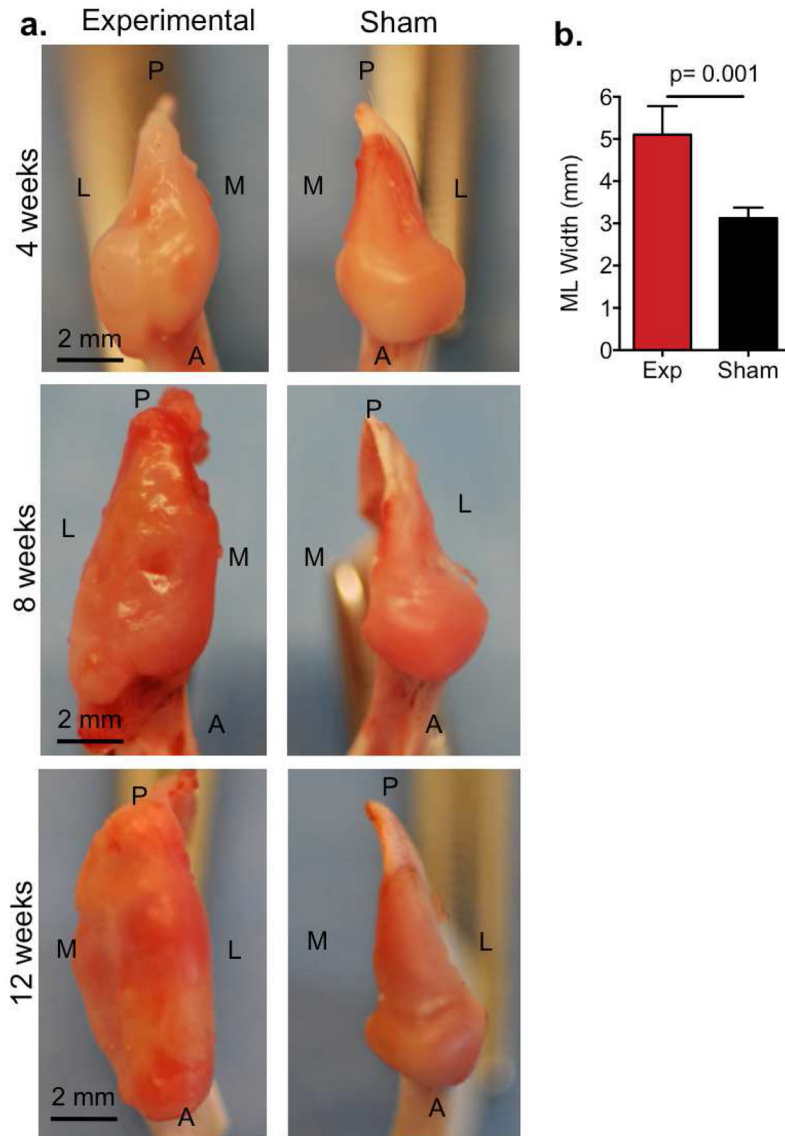
Figure 2. TMJ condyle macroscopic changes in the rabbit TMJ injury model
(a) Images are representative photographs that demonstrate the superior view of TMJ condyle at 4, 8 and 12 weeks following disc perforation surgery. Experimental TMJ disc perforation surgery was performed on left TMJs (left panels) and sham surgery was performed on the right TMJs within the same animal (right panels). P=posterior, A=anterior, L=lateral and M=medial. Scale bar = 2mm. *(b)* The medial to lateral (ML) width of the TMJ condyle was measured using Nis-Elements Basic Research imaging on experimental TMJs (exp) in comparison to sham TMJs. Data reported are reported as mean of 9 rabbits per group with 95% confidence intervals. Resulting two-tailed P-value =0.001 (exp vs sham) was regarded as statistically significant difference using paired Students t-test.
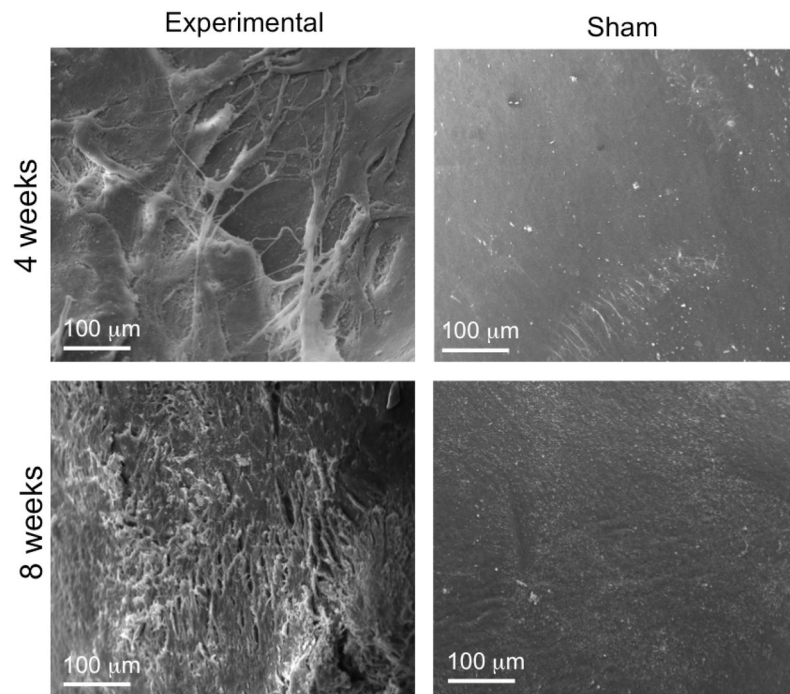
Figure 3. Scanning electron microscopy imaging of TMJ condyle surface in experimental and sham samples

SEM shows the surface of TMJ condyle at 4 weeks and 8 weeks after surgery. Experimental TMJ condyle demonstrated irregular, fibrous surface relative to smooth surface on sham TMJ condyle at both 4 and 8 weeks after surgery. Scale bar= 100 μm.
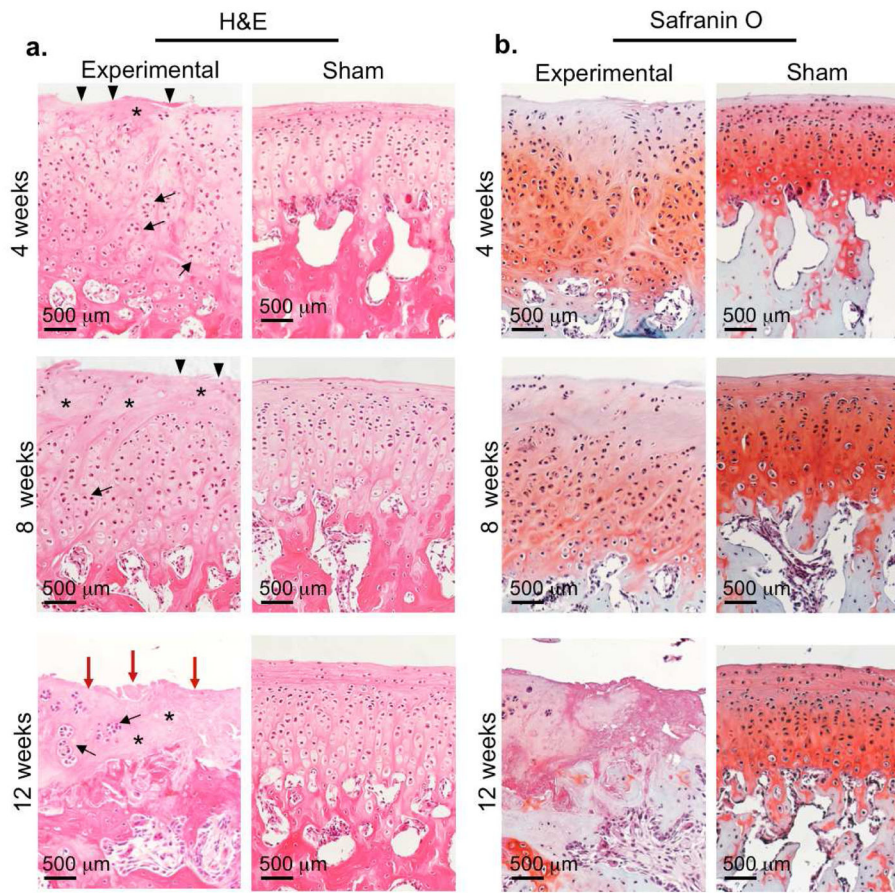
Figure 4. Histological sections of TMJ condyles in rabbit TMJ injury model
Images are representative of H&E (***a***) and safranin O (***b***) staining of TMJ condyles from experimental disc perforation side (left panels) and sham control side (right panels) at 4, 8 and 12 weeks after disc perforation surgery within comparable, middle-anterior ondylar regions. Scale bar = 500 µm. Triangles=surface irregularity; asterisks=acellular regions; black arrows=cell clusters; red arrows=erosion.
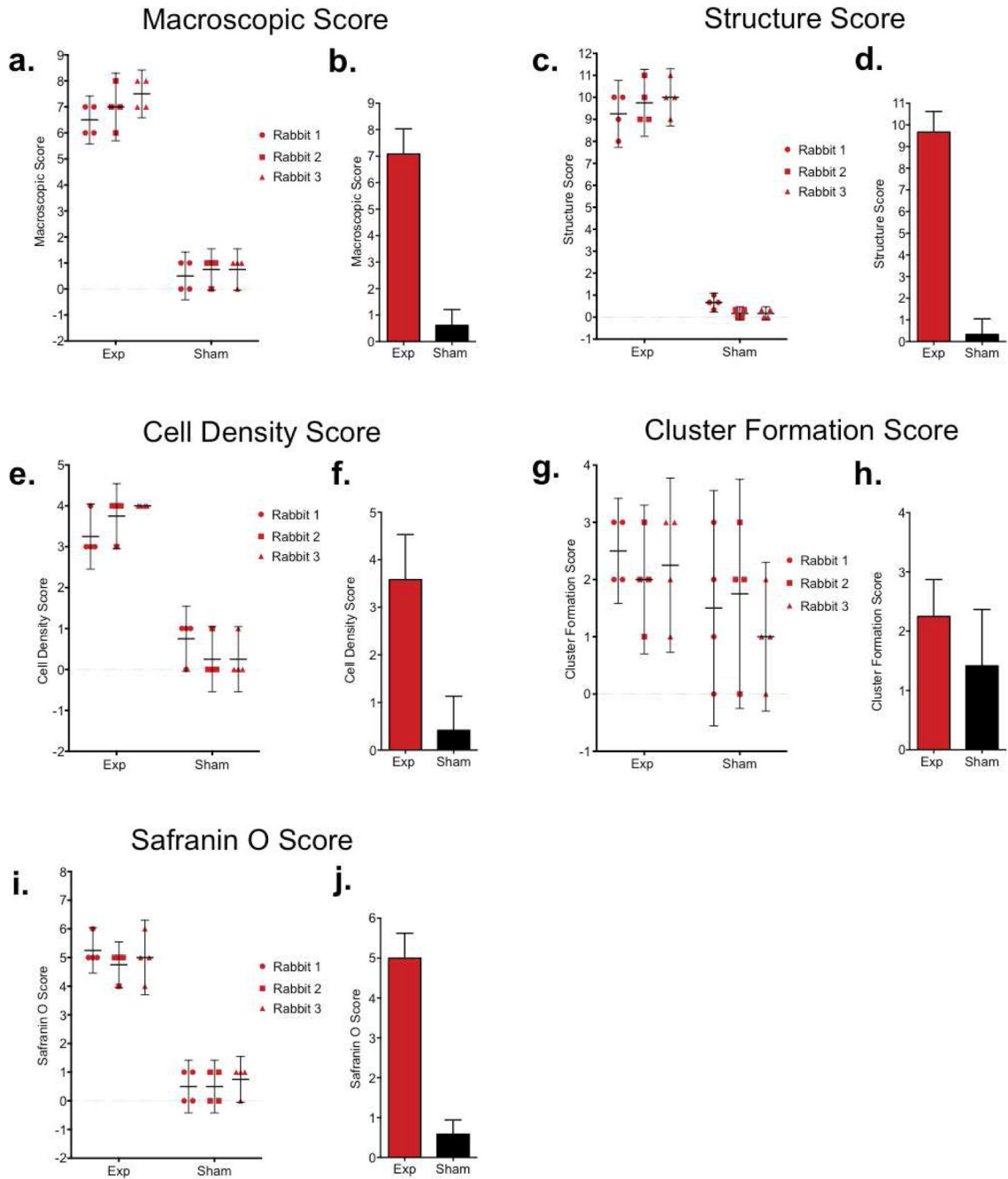
Figure 5. Histopathological scoring of TMJ condyles 12 weeks following disc perforation surgery
12 weeks after TMJ disc perforation surgery, the gross TMJ morphology and comparable
histological sections were blindly scored by 4 observers using OARSI recommendations
based on *(a, b) gross macroscopic tissue (c, d) histological* structure, *(e, f)* chondrocyte
density, *(g, h)* cluster formation, and *(i, j)* Safranin O staining. *(d, f, h, i)* Scatter plots show
each plot representing an individual observers' score per rabbit with 95% CI upper and
lower limits (n=4 observers; circles=individual observer scores for Rabbit 1;
square=individual observer scores for Rabbit 2; triangle=individual observer scores for

rabbit 3). Individual observer score per condyle (exp and sham) are mean of 3 histological sections. Each rabbit score are a mean of 4 observer scores. Right bar graphs represent mean score in experimental *vs* sham condyles (n=3 rabbits) with 95% confidence intervals.
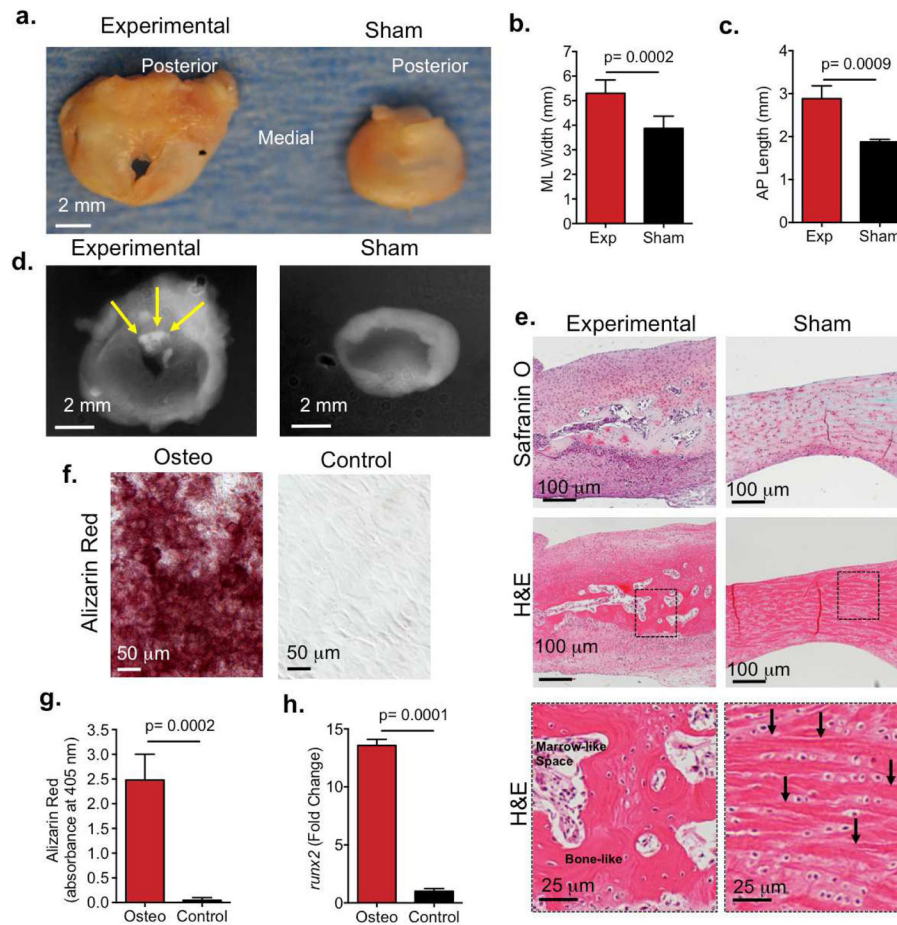
Figure 6. TMJ disc hyperplasia and heterotopic ossification in rabbit TMJ injury model
(a) Images are representative photographs that demonstrate the superior view of TMJ disc
12 weeks after surgery. TMJ disc perforation surgery was performed on left TMJs (left
panels) and sham surgery was performed on the right TMJs within the same animal (right
panels). Scale bar = 2mm. **(b–c)** The medial lateral (ML) and anterior to posterior (AP)
length of the TMJ disc was measured using Nis-Elements Basic Research imaging software
on experimental TMJs (exp) in comparison to sham TMJs. Data reported are mean of 9
rabbits per group with 95% confidence intervals; resulting two-tailed P-value   0.05 (exp vs
sham) was regarded as statistically significant difference using paired Students t-test.
experimental vs sham control. **(d)** Representative radiographs experimental (left) and sham
(right) TMJ disc showing ossified tissue (6/9 rabbits). Yellow arrow=radio-opaque tissue.
(e) Histological sections of experimental (left) and sham (right) TMJ discs (6/9 rabbits) post
surgery showed bone-like tissue formed in experimental TMJ disc. Sections were stained
with safranin O (top row) and H&E (middle and bottom row). Bottom row images are
higher magnification of dashed square box in middle row images. Arrows indicate collage
fibers. Black arrows indicate collagen fibers in sham disc. **(f)** TMJ disc cells were isolated
from New Zealand white rabbits and cultured in osteogenic media for 2 weeks. Basal
medium served as a negative control. Alizarin staining showed calcium deposition in TMJ
disc cells in osteogenic media (red, left panel). Scale bar = 50 μm. **(g)** Alizarin red staining

absorbance (405 nm). Data are normalized to cell number and are reported as a mean of 5 independent experiments with 95% confidence intervals.

(**h**) qRT-PCR showing osteogenic marker runx2 upregulated 13.5 fold in TMJ disc cells in osteogenic media. Data are normalized to GAPDH. Data are reported as mean fold change with 95% confidence intervals and are representative of 6 independent experiments.